A K-OMEGA ANALYSIS OF TURBULENT SUPERSONIC CHANNEL FLOW DNS DATA

Stefan Heinz
Department of Mathematics
University of Wyoming
1000 East University Avenue, Laramie, WY 82071, USA
heinz@uwyo.edu

Holger Foysi and Rainer Friedrich
Fachgebiet Strömungsmechanik
Technische Universität München
Boltzmannstr. 15, D-85747 Garching, Germany
holger@flm.mw.tum.de and r.friedrich@lrz.tu-muenchen.de

ABSTRACT

Statistical modeling of turbulent supersonic channel flow is considered on the basis of direct numerical simulation (DNS) data. First, the DNS data are studied within the frame of a turbulence model, this means the model parameters are calculated such that the turbulence model predictions agree with corresponding DNS data. This representation of DNS data is used to analyze the structure of the turbulence model considered for different Reynolds and Mach numbers. It is shown that standard modeling assumptions (e.g., regarding the structure of the turbulence frequency equation) are inapplicable to the flows considered. New closure models are developed, therefore, which result in a turbulence model that is optimized for a class of channel flows.

INTRODUCTION

Most of the simulations of turbulent flows are performed within the frame of Reynolds-averaged Navier-Stokes (RANS) methods. The application of more general probability density function (PDF) methods to reacting flow simulations enables the exact treatment of important processes, as, for example, chemical reactions (Pope, 2000; Fox, 2003; Heinz, 2003a). The reason for the predominant use of RANS and PDF methods is given by the fact that their computational costs are much lower than those of large eddy simulation and filter density function methods. However, the relative simplicity of RANS and PDF methods is also the reason for some significant problems, which limit their accuracy.

A first problem arises from the fact that there are good concepts available to model the evolution of velocity and scalar fields, but all these models have to be combined with a transport equation for the turbulence frequency ω (or dissipation rate $\varepsilon = k\,\omega$ of the turbulent kinetic energy k) which determines the characteristic time scale $\tau = 1 / \omega$ of turbulent motions. Unfortunately, the basis for constructing an equation for ω is weak because the most important term in this equation, the standardized source rate S_ω, is unknown (Pope, 2000; Wilcox, 1998).

A second problem is related to the optimization of the performance of turbulence models (Pope, 1999). The relative efficiency of turbulence models mainly arises from the fact that turbulence model parameters (as, e.g., C_μ, see below) are introduced via the parametrization of correlations of turbulent velocities and scalars which appear as unknowns in turbulence models. Originally, such model parameters were assumed to be constant (Launder, 1990), but many investigations indicated significant shortcomings as a consequence of this assumption. This concerns, in particular, the modeling of wall-bounded flows, which is relevant to most of the applications. It turned out that the performance of turbulence models for such flows can be significantly improved by introducing varying turbulence model parameters, so that the damping effect of walls can be taken into account. However, concepts applied previously to handle this question are hardly supported by DNS data (Rodi and Mansour, 1993).

A third problem concerns the development of solutions for the two problems described above (or, more general, the development of turbulence models) with regard to variable-density flows, which is relevant to turbulent combustion calculations (Friedrich, 1999; Chassaing et al., 2002). Compressibility effects that were observed in such flows may be differentiated into dilatational and structural effects. Dilatational compressibility effects of about 10% were observed in homogeneous shear flows (Sarkar, 1995), but their relevance to wall-bounded flows appears to be extremely low (Friedrich, 1999). In contrast to that, structural compressibility effects (i.e., changes of the dimensionless anisotropy tensor due to a reduction of the turbulent kinetic energy redistribution) were found to have a very significant effect on the production and dissipation of turbulence in homogeneous shear flows (Sarkar, 1995), which requires corresponding modifications of turbulence models (Heinz, 2003b). With regard to wall-bounded flows there is certainly the need for further investigations of the significance of these effects and of appropriate ways to incorporate them in turbulence models.

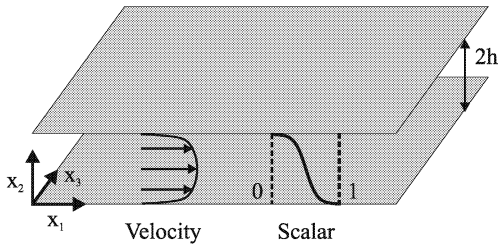

Fig. 1. A sketch of the channel flow considered. h refers to the half channel height. Mean velocity and scalar profiles appear only in wall-normal direction x_2.

The three problems described above will be addressed here by adopting recently obtained DNS data of supersonic channel flow at different Reynolds and Mach numbers (Foysi et al. 2004). The investigations will be performed in the following way. In a first step, the DNS data are considered within the frame of a turbulence model, this means its parameters will be calculated such that the predictions of the turbulence model agree with the corresponding DNS data. In a second step, the spatial distributions of turbulence model parameters obtained in this way will be used to derive parametrizations that may be applied in turbulence models. The suitability of such approximations is then investigated by applying them in simulations and comparing the results with DNS data.

DIRECT NUMERICAL SIMULATION

Compressible flow of air through a channel of infinitely large plates (with a wall distance of 2 h) is considered, see Fig. 1. The flow is driven by a uniform body force. No-slip and impermeability conditions are applied to the velocity field at the walls, and periodic boundary conditions are used in stream- and spanwise directions. Both channel walls are cooled and kept at constant temperature so that there is heat transfer out of the channel allowing supersonic fully-developed flow. A passive scalar is injected at the lower wall and removed at the upper wall (Foysi et al. 2004).

The flow dynamics are described by the compressible Navier-Stokes equations for the mass density ρ, velocity U_i ($i = 1, 3$), temperature T and mass fraction m of a passive scalar,

$$\frac{D\rho}{Dt} = -\rho S_{kk}, \tag{1a}$$

$$\frac{DU_i}{Dt} = \frac{2}{\rho}\frac{\partial}{\partial x_k}\mu S^d_{ik} - \frac{1}{\rho}\frac{\partial p}{\partial x_i} + \frac{1}{\rho}\left(f + \frac{\partial < p >}{\partial x_1}\right)\delta_{i1}, \tag{1b}$$

$$\frac{DT}{Dt} = \frac{1}{\rho}\frac{\partial}{\partial x_k}\frac{\gamma\mu}{Pr}\frac{\partial T}{\partial x_k} - (\gamma - 1)S_{kk}T + \frac{\mu s^2}{\rho c_v}, \tag{1c}$$

$$\frac{Dm}{Dt} = \frac{1}{\rho}\frac{\partial}{\partial x_k}\frac{\mu}{Sc}\frac{\partial m}{\partial x_k}. \tag{1d}$$

Here, $D / Dt = \partial / \partial t + U_k \, \partial / \partial x_k$ and $s = (2S^d_{ik}S^d_{ki})^{1/2}$, where S_{ik}^d represents the deviatoric part of the rate-of-strain tensor $S_{ik} = (\partial U_i / \partial x_k + \partial U_k / \partial x_i) / 2$. δ_{ij} represents the Kronecker delta and the sum convention is applied throughout this paper. The pressure p is given by the thermal equation of state $p = \rho R T$, where R refers to the gas constant. In equation (1b), a force $f = \tau_w / h$ is introduced (τ_w represents the wall shear stress) which replaces the ensemble-averaged pressure gradient $\partial <p> / \partial x_1$.

The closure of the equations (1b)-(1d) requires the definition of molecular properties. For the dynamic viscosity we use $\mu = \mu_w (T / T_w)^{0.7}$, where μ_w and T_w refer to wall values of viscosity and temperature, respectively. The Prandtl number is Pr = 0.7 and the Schmidt number Sc = 1.0. The ratio $\gamma = c_p / c_v$ of specific heats at constant-pressure and constant-volume, respectively, is given by $\gamma = 1.4$, and the gas constant $R = c_p - c_v = 287$ J / (kg K). This implies $c_p = \gamma R / (\gamma - 1)$.

All the details of the solution of the equations (1a)-(1d) may be found elsewhere (Foysi et al. 2004). The stationary ensemble (Reynolds) and mass density-weighted (Favre) means considered below were obtained by averaging over the homogeneous stream- and spanwise directions. The ensemble mean of any quantity Q is denoted by <Q> whereas an overbar refers to a mass density-weighted mean, $\overline{Q} = <\rho Q> / <\rho>$.

Simulations were performed by adopting the boundary conditions described above for three sets of the friction Reynolds number Re_τ, bulk Reynolds number Re_0 and Mach number M_0. These parameters are defined by

$$Re_\tau = \frac{\rho_w u_\tau h}{\mu_w}, \qquad Re_0 = \frac{\rho_0 u_0 h}{\mu_w}, \qquad M_0 = \frac{u_0}{a_w}. \tag{2}$$

They may be seen as dimensionless measures for the friction velocity, bulk velocity and sound velocity at the wall. These velocities are given by

$$u_\tau = \sqrt{\frac{\tau_w}{\rho_w}}, \qquad u_0 = \frac{1}{h}\int_0^h dx_2 \overline{U}_1, \qquad a_w = \sqrt{\gamma R T_w}. \tag{3}$$

In these expressions, ρ_w is the wall mass density and ρ_0 is the bulk mass density which is defined in correspondence to u_0. The values for Re_τ, Re_0 and M_0 considered in this way are presented in Table 1, and characteristic simulation data are given in Table 2. The IL data agree well with DNS data of Moser et al. (1999).

As may be seen in Table 1, the cases IL, CL and CH differ by growing Reynolds and Mach numbers Re_τ, Re_0 and M_0. However, these parameters do not reflect local flow characteristics. This may be seen by considering the local Reynolds number Re and Mach number M,

$$Re = \frac{\overline{U}_1 h}{\overline{\nu}}, \qquad M = \frac{\overline{U}_1}{a}. \tag{4}$$

Here, $\overline{U}_1$ is the mean streamwise velocity, $a = (\gamma R \overline{T})^{1/2}$ refers to the mean speed of sound, and $\overline{\nu} = <\mu> / <\rho>$ is the mean kinematic viscosity. The corresponding curves of Re and M are given in Figs. 2a-b. These figures show that the local Reynolds numbers of IL and CL and the local Mach numbers of CL and CH are basically the same. Hence, the comparison of IL and CL shows the Mach number effect whereas the Reynolds number effect follows from the comparison of CL and CH.

Case	Re_c	M_c	Re_τ	Re_0	M_0
IL = incomp., low-Re	3300	0.4	181	2820	0.3
CL = comp., low-Re	3400	2.2	556	6000	3.0
CH = comp., high-Re	6100	2.2	1030	11310	3.5

Table 1. The centerline Reynolds number Re_c, centerline Mach number M_c, friction Reynolds number Re_τ, bulk Reynolds number Re_0 and Mach number M_0.

The turbulence may be characterized by the turbulence Reynolds number Re_L, turbulence Mach number M_t and gradient Mach number M_g. These numbers are defined by

$$Re_L = \frac{k^2}{\varepsilon\bar{\nu}}, \qquad M_t = \frac{\sqrt{2k}}{a}, \qquad M_g = \frac{S\Delta_g}{a}. \tag{5}$$

Here, $k = \overline{u_i u_i} / 2$ refers to the turbulent kinetic energy (turbulent velocity fluctuations are denoted by u_i where i = 1, 3) and ε is the dissipation rate of k. ε is often considered as the sum of solenoidal (ε_s) and dilatational (ε_d) contributions, $\varepsilon = \varepsilon_s + \varepsilon_d$. However, there is no need for doing this here because dilatational contributions are very small: one finds $\varepsilon_d / \varepsilon_s < 0.001$. The characteristic mean shear rate $S = \bar{s}$ is used in the definition of M_g, and Δ_g is a characteristic length scale of turbulence in the direction of shear. Δ_g is defined by $\Delta_g = \kappa (h - |x_2 - h|)$, where $\kappa = 0.4$ refers to the von-Karman constant. The corresponding curves for Re_L, M_t and M_g are given in Figs. 2c-d. These figures reveal features which correspond to those given in Figs. 2a-b: The turbulence Reynolds numbers of IL and CL and the turbulence Mach numbers of CL and CH are very similar. By adopting $Re_\lambda = (20\, Re_L / 3)^{1/2}$ for the relation between Re_L and the Taylor-scale Reynolds number Re_λ, one finds $25 \le Re_\lambda \le 44$ (except very close to the walls), which is of the same order as values given with regard to corresponding investigations of homogeneous shear flows. The turbulence Mach number M_t and gradient Mach number M_g are small compared to values observed in homogeneous shear flows (Sarkar, 1995).

Case	N_1	N_2	N_3	L_1 / h	L_2 / h	L_3 / h
IL	192	129	160	9.6	2	6
CL	512	221	256	4π	2	$4\pi / 3$
CH	512	301	256	6π	2	$4\pi / 3$

Case	Δx_1^+	$\Delta x_2^+{}_{min}$	$\Delta x_2^+{}_{max}$	Δx_3^+
IL	9.12	1.02	4.21	6.84
CL	13.65	0.89	9.38	8.91
CH	37.89	1.27	13.35	16.85

Table 2. Simulation data for the IL, CL and CH cases considered. N_1, N_2 and N_3 are the number of grid points in x_1-, x_2-, x_3-directions. L_1, L_2 and L_3 are the corresponding domain lengths. Δx_1^+, Δx_2^+ and Δx_3^+ refer to the node distance normalized on the viscous length scale $\delta_\nu = \nu_w / u_\tau$ (the minimal and maximal values of Δx_2^+ are given).

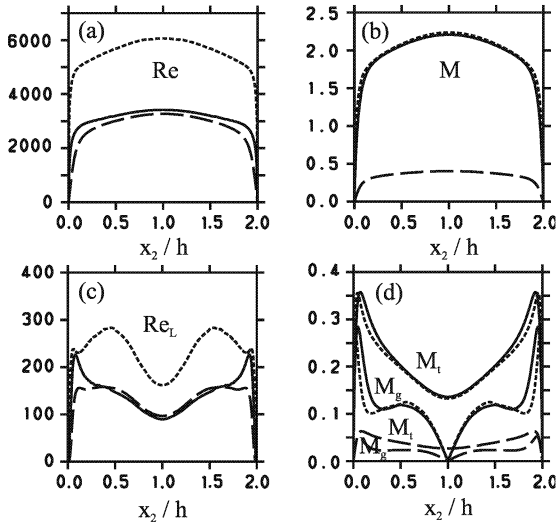

Fig. 2. DNS data for the (a) local Reynolds number Re, (b) local Mach number M, (c) turbulence Reynolds number Re_L, (d) turbulence Mach number M_t and gradient Mach number M_g against the normalized wall-normal coordinate x_2 / h (IL: ——; CL: ——; CH: - - - -).

Basic flow characteristics are given in Fig. 3. The normalized production $P / (S k) = |\overline{u_1 u_2}| / k$ and inverse dissipation $S k / \varepsilon = S \tau$ of turbulent kinetic energy k are shown in Figs. 3a-b. In homogeneous shear flows, both the quantities $P / (S k)$ and $S \tau$ were found to be primarily affected by structural compressibility effects: they scale with the gradient Mach number (Heinz, 2003b). For the wall-bounded flows considered here, the influence of structural compressibility effects is much lower. Compared to the IL case, $P / (S k)$ is somewhat smaller for CL. This finding agrees with the trend observed for homogeneous shear flows, but this effect is very small. With regard to $S \tau$ there is no observable compressibility effect. In contrast to that one finds for both $P / (S k)$ and $S \tau$ a stronger Reynolds number effect: the normalized production $P / (S k)$ and dissipation rate $\varepsilon / (S k)$ increase.

Corresponding features for the production-to-dissipation ratio P / ε of turbulent kinetic energy may be observed in Fig. 3c: there is hardly a compressibility effect but a higher Reynolds number has a stronger effect (the plateau region is more pronounced, this means a higher Re implies a larger local-equilibrium region). Alternatively to the time scale ratio $S \tau$, one may consider a similar length scale ratio (which may be seen as a characteristic eddy length scale) $\ell_* = \tau\, k^{1/2} / (2 h)$ to asses the relevance of compressibility effects. Theoretical estimates suggest $\ell_* \approx 1 / 3$ (Heinz, 2003a). Fig. 3d shows that this estimate agrees well with the values observed here. ℓ_* is affected by both Reynolds and Mach number effects. Compressibility leads to a somewhat more homogeneous spatial distribution of ℓ_* (a higher near-wall peak and lower centerline value) whereas a higher Reynolds number has the opposite effect.

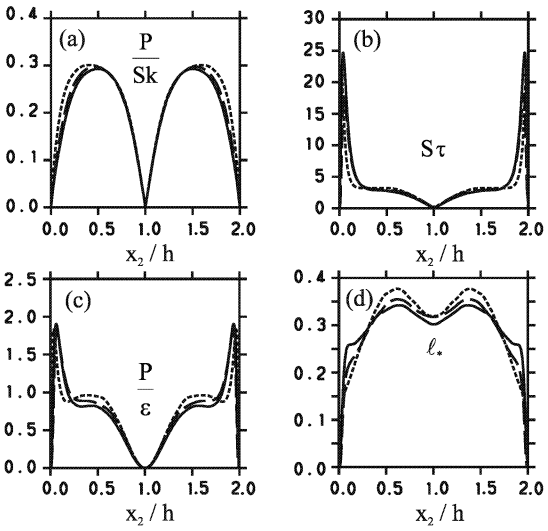

Fig. 3. DNS data for the (a) normalized production P / (S k) of k, (b) normalized inverse dissipation S k / ε = S τ, (c) production-to-dissipation ratio P / ε of k and (d) characteristic eddy length scale ℓ_*.

A K-OMEGA ANALYSIS OF DNS DATA

The DNS data described in the previous section will be considered now within the frame of a turbulence model, i.e., the turbulence model parameters will be calculated such that the model predictions agree with the corresponding DNS data. There are several ways to realize such an analysis. The averaging of the equations (1a)-(1d) reveals that one has to provide closures, for example, for the Reynolds stress tensor, turbulent heat and mass flux. Such closures can be obtained on the basis of transport equations for these quantities, or, by the further reduction of these transport equations to algebraic expressions for these quantities. The latter way, which represents the natural first step of such an analysis, will be applied here.

In particular, we will apply a k-ω turbulence model. Compared to a k-ε model, this model has the advantage that it can be applied well into the viscous sub-layer, while the k-ε model (with wall functions) requires the first grid point away from the wall to lie in the log layer (Fox, 2003; Wilcox 1998). By adopting algebraic approximation for turbulent fluxes (Pope, 2000; Fox, 2003; Heinz, 2003a), the transport equations for the ensemble-averaged mass density $\langle\rho\rangle$ and mass density-weighted velocities $\overline{U}_i$, temperature $\overline{T}$ and mass fraction $\overline{m}$, respectively, are given by

$$\frac{\overline{D}\langle\rho\rangle}{\overline{D}t} = -\langle\rho\rangle\overline{S}_{kk}, \tag{6a}$$

$$\frac{\overline{D}\,\overline{U}_i}{\overline{D}t} = \frac{2}{\langle\rho\rangle}\frac{\partial}{\partial x_k}\left(<\mu>+\mu_T\right)\overline{S}_{ik}^{\,d} - \frac{\partial\left(\langle p\rangle + 2\langle\rho\rangle k/3\right)}{\langle\rho\rangle\partial x_i} + \frac{1}{\langle\rho\rangle}\left(f + \frac{\partial\langle p\rangle}{\partial x_1}\right)\delta_{i1}, \tag{6b}$$

$$\frac{\overline{D}\,\overline{T}}{\overline{D}t} = \frac{1}{\langle\rho\rangle}\frac{\partial}{\partial x_k}\gamma\left(\frac{<\mu>}{Pr}+\frac{\mu_T}{Pr_t}\right)\frac{\partial\overline{T}}{\partial x_k} - (\gamma-1)\overline{S}_{kk}\overline{T} + \frac{\varepsilon}{c_v} + \frac{1}{c_v}\overline{\nu}S^2, \tag{6c}$$

$$\frac{\overline{D}\,\overline{m}}{\overline{D}t} = \frac{1}{\langle\rho\rangle}\frac{\partial}{\partial x_k}\left(\frac{<\mu>}{Sc}+\frac{\mu_T}{Sc_t}\right)\frac{\partial\overline{m}}{\partial x_k}. \tag{6d}$$

Here, $\overline{D}/\overline{D}t = \partial/\partial t + \overline{U}_k\,\partial/\partial x_k$ and $\langle p\rangle = \langle\rho\rangle R\,\overline{T}$. Pr_t and Sc_t refer to the turbulence Prandtl and Schmidt numbers, respectively. For the turbulent viscosity μ_T we apply the parametrization $\mu_T = C_\mu \langle\rho\rangle k/\omega$. Here, C_μ is a parameter that has to be calculated and $\omega = 1/\tau = \varepsilon/k$ refers to the turbulence frequency. It is assumed that the turbulent kinetic energy k and ω obey the equations

$$\frac{\overline{D}k}{\overline{D}t} = \frac{1}{\langle\rho\rangle}\frac{\partial}{\partial x_k}\left(<\mu>+\frac{\mu_T}{Pr_k}\right)\frac{\partial k}{\partial x_k} + C_\mu S^2\frac{k}{\omega} - k\omega, \tag{7a}$$

$$\frac{\overline{D}\omega}{\overline{D}t} = \frac{1}{\langle\rho\rangle}\frac{\partial}{\partial x_k}\left(<\mu>+\frac{\mu_T}{Pr_\omega}\right)\frac{\partial\omega}{\partial x_k} - S_\omega\omega^2. \tag{7b}$$

Here, Pr_k and Pr_ω are Prandtl numbers. S_ω refers to the source rate in the turbulence frequency equation, which is usually parametrized by the expression (Wilcox, 1998)

$$S_\omega = \alpha_2 - \alpha_1\frac{C_\mu S^2}{\omega^2}. \tag{8}$$

α_1 and α_2 are parameters that have to be calculated. $C_\mu S^2/\omega^2$ represents the modeled production-to-dissipation ratio of turbulent kinetic energy, see equation (7a). Regarding the structure of the equations (7a)-(7b) it is worth noting that the mean dilatation is negligible for the flow considered. In correspondence to the negligible influence of dilatational dissipation effects one finds that the contribution of the pressure dilatation $\Pi_d = \overline{(p/\rho)"S_{kk}"}$ is extremely small: we have $|\Pi_d/(\langle\rho\rangle\varepsilon)| < 0.008$.

By adopting the DNS data presented above in the equations (6b)-(6d) and (7a), one can calculate the model parameters C_μ, Pr_t, Sc_t and Pr_k, respectively. To calculate Pr_ω and S_ω, we have only one relation available: equation (7b). Thus, we assume (in consistency with the treatment of Pr_t, Sc_t and Pr_k described below) that Pr_ω is constant. Equation (7b) can be applied then for the calculation of S_ω in dependence on values chosen for Pr_ω.

The model parameters calculated in this way are shown in Fig. 4. C_μ, which is often approximated by $C_\mu = 0.09$ (Pope, 2000; Wilcox, 1998), shows significant variations with the normalized wall distance x_2/h. The Mach number increase implies a somewhat higher standardized turbulent transport efficiency C_μ, which appears to be plausible. The Reynolds number increase has a significant effect: the CH plateau is much more pronounced than for the IL and CL cases. This behaviour is similar to the features found for the production-to-dissipation ratio P / ε and S τ, see Fig. 3.

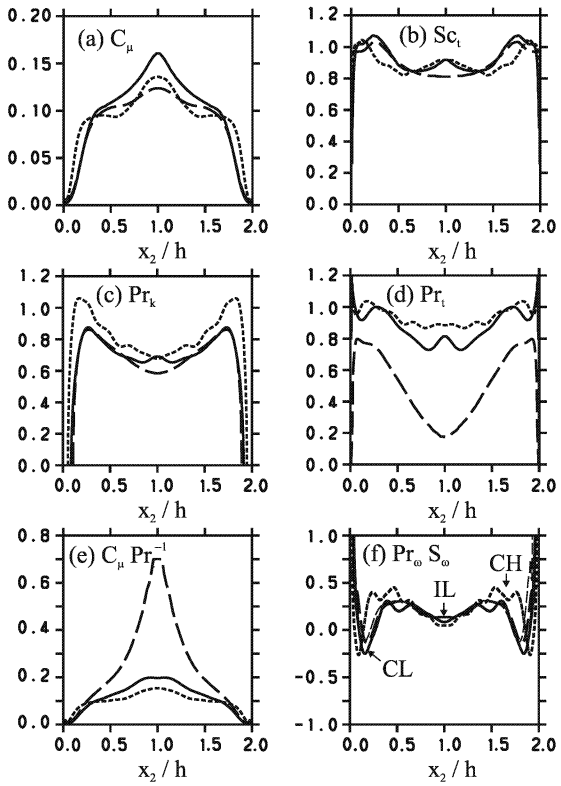

Fig. 4. DNS data for the turbulence model parameters (a) C_μ, (b) Sc_t, (c) Pr_k, (d) Pr_t and (e) C_μ / Pr_t. $Pr_\omega\ S_\omega$ is shown according to (7b) in (f), where two values for Pr_ω are applied: $Pr_\omega = 0.6$ and $Pr_\omega = 0.9$.

The results found for the dimensionless numbers Sc_t, Pr_k and Pr_t reveal the following. The effect of compressibility is small with regard to Sc_t and Pr_k, but there is a relevant influence on Pr_t: the stronger coupling of the transport of momentum and heat in compressible flows hampers, therefore, the standardized turbulent energy transport efficiency C_μ / Pr_t. The Reynolds number has a similar effect on Pr_k and Pr_t: their values are closer to unity, this means the difference between the turbulent transport of turbulent kinetic energy and temperature to the turbulent momentum transport becomes smaller. The effect of the Reynolds number on Sc_t is smaller than its effect on Pr_k and Pr_t, which may be related to the fact that the IL and CL values for Sc_t are already close to unity.

$Pr_\omega\ S_\omega$ is shown according to (7b) where $Pr_\omega = 0.6$ and $Pr_\omega = 0.9$ are applied (which corresponds to an appropriate range of variations). A relevant (and somewhat surprising) finding is that the compressibility effect on $Pr_\omega\ S_\omega$ is rather small, this means compressibility does not affect the generation mechanism of turbulence frequency. In contrast to that, the Reynolds number increase has a significant structural effect: the source rate distribution becomes smoother. This feature agrees again well with similar findings for the production-to-dissipation ratio P / ε, time scale ratio $S\,\tau$ and C_μ.

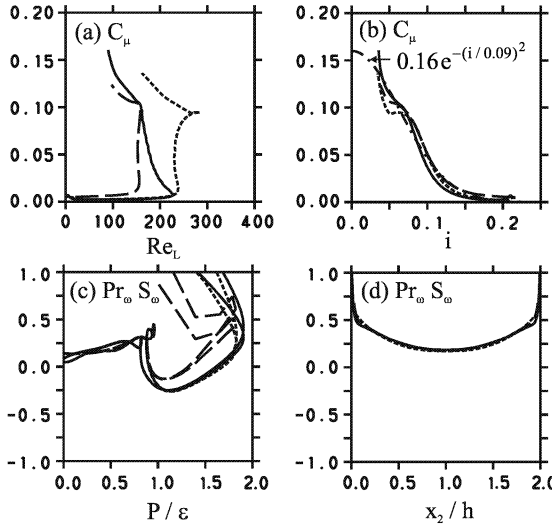

Fig. 5. DNS data for C_μ are plotted (with the same line coding as above) in (a) against the turbulence Reynolds number Re_L and (b) turbulence intensity i. $Pr_\omega\ S_\omega$ is plotted in (c) against the production-to-dissipation ratio P / ε of k, where $Pr_\omega = 0.9$ and $Pr_\omega = 0.6$ are applied. In (d), $Pr_\omega\ S_\omega$ is shown against x_2 / h, where the approximation $Pr_\omega\ S_\omega = (0.34 - 0.54\,\tau_*) / \tau_*^{0.22}$ is used.

TURBULENCE MODELING

The findings obtained for the turbulence model parameters can be used as guideline for the development of a turbulence model, which requires parametrizations of model parameters in terms of quantities that are available in simulations. Such an analysis reveals that the use of the effective value $Pr_t = Pr_k = Pr_\omega = Sc_t = 0.9$ for the dimensionless numbers in the temperature, turbulent kinetic energy, frequency and scalar equations is well justified (Heinz et al., 2005). No support is found for the usual practice of modeling C_μ and S_ω: C_μ does not scale with the turbulence Reynolds number Re_L, and the model (8) disagrees with the DNS results, see Figs. (5a) and (5c). With regard to C_μ one finds instead that the parametrization $C_\mu = 0.16 \exp(-[i / 0.09]^2)$ works very well (see Fig. 5b), where $i = (2\,k / 3)^{1/2} / \overline{U}_1$ refers to the turbulence intensity. An analysis of (7b) shows that $Pr_\omega\ S_\omega$ may be well approximated by $Pr_\omega\ S_\omega = (0.34 - 0.54\,\tau_*) / \tau_*^{0.22}$ (Heinz et al., 2005), where $\tau_* = (\tau_w / \rho)^{1/2}\,\tau / (2h)$ represents a dimensionless time scale. Fig. 5d shows the corresponding variation of $Pr_\omega\ S_\omega$.

The FLUENT code (Fluent, 2003) was adopted to realize flow simulations with the turbulence model described above (all the details may be found in Heinz et al. (2005)). As may be seen in Fig. 6, the performance of the resulting turbulence model is very good: there are hardly differences to the DNS results. With regard to the variations of S_ω it is worth noting that the use of a constant value $S_\omega = 0.75$ still results in good model predictions: the deviations between model results and DNS are stronger, but the structures of k and ε are still well represented.

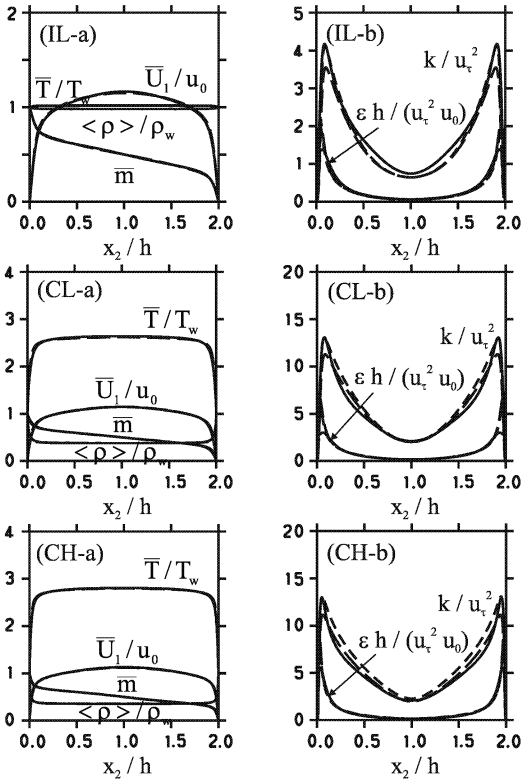

Fig. 6. A comparison of DNS data (solid lines) with model predictions. For the three cases considered, the normalized mean streamwise velocity, temperature, mass density and scalar are given in Figs. (a) against the normalized wall-normal coordinate x_2 / h. The model predictions are only shown for $Pr_\omega = 0.9$ (line ——) because there is no difference to the corresponding results for $Pr_\omega = 0.6$. The DNS data and model predictions for the normalized turbulent kinetic energy k and its dissipation rate ε are given in Figs. (b), where the $Pr_\omega = 0.9$ results are compared to corresponding $Pr_\omega = 0.6$ (line – – –) results.

CONCLUSIONS

This analysis results in the following conclusions. Mach number effects on the turbulence characteristics considered are small. A Reynolds number increase has a stronger influence: it causes larger flow regions that may be considered to be in a local equilibrium. The relevance of both Reynolds and Mach numbers on the turbulence model considered, however, is insignificant: constant Prandtl numbers and parametrizations of S_ω and C_μ which are hardly affected by Reynolds and Mach number variations may well explain the structure of the flows considered. Nevertheless, standard modeling assumptions regarding the structure of the turbulence frequency equation and variation of model parameters were found to be inapplicable to the flows considered. Thus, new closure models were developed. The result is a turbulence model that is optimized for a class of channel flows.

Acknowledgement

This work was supported by the German Research Foundation (DFG, SFB 255, TP A2 and FR 478/20-2) and Fluent Germany (Dr. M. Braun) as part of a program related to the development of improved numerical methods for turbulent combustion. We are thankful to J. Kreuzinger for helpful suggestions and support regarding the comparisons with DNS data.

REFERENCES

Chassaing, P., Antonia, R. A., Anselmet, F., Joly, L. and Sarkar, S., 2002, "Variable Density Fluid Turbulence", Fluid Mechanics and its Applications 69, Kluwer Academic Publishers, Dordrecht, Boston, London.

FLUENT Inc., 2003, "FLUENT 6.1 User's Guide", Lebanon, New Hampshire, USA .

Fox, R. O., 2003, "Computational Models for Turbulent Reacting Flows", Cambridge Series in Chemical Engineering, Cambridge University Press, Cambridge.

Foysi, H., Sarkar, S. and Friedrich, R., 2004, "Compressibility Effects and Turbulence Scalings in Supersonic Channel Flow", J. Fluid Mech. 509, 207-216.

Friedrich, R., 1999, "Modelling of Turbulence in Compressible Flows", In: Transition, Turbulence and Combustion Modelling, edited by Hanifi, A., Alfredsson, P. H., Johansson, A. V. and Henningson, D. S., Kluwer Academic Publishers (ERCOFTAC Series), Dordrecht, Boston, London, 243-348.

Heinz, S., 2003a, "Statistical Mechanics of Turbulent Flows", Springer-Verlag, Berlin, Heidelberg, New York.

Heinz, S., 2003b, "A Model for the Reduction of the Turbulent Energy Redistribution by Compressibility", Phys. Fluids 15, 3580-3583.

Heinz, S., Foysi, H. and Friedrich, R., 2005, "Turbulent Supersonic Channel Flow: Statistical Modeling based on Direct Numerical Simulation Data", (submitted).

Launder, B. E., 1990, "Phenomenological Modeling: Present and Future", In: Wither Turbulence? Turbulence at the Crossroads, edited by Lumley, J. L., Springer-Verlag, Berlin, 439-485.

Moser, R. D., Kim, J. and Mansour, N. N., 1999, "Direct Numerical Simulation of Turbulent Channel Flow up to $Re_\tau = 590$", Phys. Fluids 11, 943-945.

Pope, S. B., 1999, "A Perspective on Turbulence Modeling", In: Modeling Complex Turbulent Flows, edited by Salas, M. D., Hefner, J. N. and Sakell, L., Kluwer, 53-67.

Pope, S. B., 2000, "Turbulent Flows", Cambridge University Press, Cambridge.

Rodi, W. and Mansour, N. N., 1993, Low Reynolds Number k-ε Modelling with the Aid of Direct Numerical Simulation Data. J. Fluid Mech. 250, 509-529.

Sarkar, S., 1995, "The Stabilizing Effect of Compressibility in Turbulent Shear Flow", J. Fluid Mech. 282, 163-186.

Wilcox, D. C., 1998, "Turbulence Modeling for CFD", Second edition, DCW Industries, Inc.